The contribution of two-nucleon emission clearly goes in the right direction, but seems to be too small. We therefore tend to conclude that a yet unknown mechanism is responsible for the pronounced strength between quasielastic and Δ peaks systematically observed in this experiment.

In the above discussion, we have limited ourselves to the dip region. The quantitative interpretation of the entire longitudinal and transverse response function—a quantity for which systematical experimental information hardly exists in the litterature—will be considered elsewhere.

The external users of the Saclay Laboratory thank P. Catillon and the staff of the Département de Physique Nucléaire et Hautes Energies for the hospitality extended to them during this work. We thank T. de Forest, Jr., G. Do Dang, and T. W. Donnelly for very stimulating discussions. This work was supported in part by the Research Corporation, the U. S. National Science Foundation, and the Swiss National Science Foundation.

[1]R. R. Whitney, I. Sick, J. R. Ficenec, A. D. Kephart, and W. P. Trower, Phys. Rev. C 9, 2230 (1974).

[2]P. D. Zimmerman, J. M. Finn, C. F. Williamson, T. de Forest, Jr., and W. C. Hermans, to be published.

[3]A. E. L. Dieperink, T. de Forest, Jr., I. Sick, and R. A. Brandenburg, Phys. Lett. 63B, 261 (1976).

[4]K. Nakamura, S. Hiramatsu, T. Kamae, A. Muramatsu, N. Izutsu, and Y. Watase, Nucl. Phys. A268, 381 (1976).

[5]J. Mougey, M. Bernheim, A. Bussière, A. Gillebert, Phan Xuan Ho, M. Priou, D. Royer, I. Sick, and G. J. Wagner, Nucl. Phys. A262, 461 (1976).

[6]P. Leconte, thesis, University of Paris XI, 1976 (unpublished).

[7]J. Mougey, thesis, University of Paris XI, 1976 (unpublished).

[8]M. Bourdinaud, J. B. Cheze, and J. C. Thevenin, Nucl. Instrum. Methods 136, 99 (1976).

[9]I. Sick and J. S. McCarthy, Nucl. Phys. A150, 631 (1970).

[10]L. W. Mo and Y. S. Tsai, Rev. Mod. Phys. 41, 205 (1969).

[11]G. Miller, SLAC Report No. 129, 1971 (unpublished).

[12]L. C. Maximon and D. B. Isabelle, Phys. Rev. 133, 1344 (1964).

[13]E. Borie, Lett. Nuovo Cimento 1, 106 (1971).

[14]T. de Forest, Jr., Nucl. Phys. A132, 305 (1969).

[15]T. Janssens, R. Hofstadter, E. B. Hughes, and M. R. Yearian, Phys. Rev. 142, 922 (1966).

[16]E. Borie, in *Proceedings of the Seventh International Conference on High-Energy Physics and Nuclear Structure, Zurich, 1977* (Schweizerisches Institut für Nuklearforschung, Villigen, 1977), p. 247.

[17]G. Do Dang, Phys. Lett. 69B, 425 (1977), and private communication.

[18]K. Stanfield, C. Canizares, W. Faissler, and F. M. Pipkin, Phys. Rev. C 3, 1448 (1971).

[19]T. W. Donnelly, J. W. van Orden, T. de Forest, Jr., and J. C. Hermans, Phys. Lett. 76B, 393 (1978); T. de Forest, Jr., private communication.

Observation of Pair Splittings in the Autoionization Spectrum of Ba

W. E. Cooke and T. F. Gallagher
Molecular Physics Laboratory, SRI International, Menlo Park, California 94025
(Received 11 September 1978)

Using a three-step laser-excitation process we have selectively excited each of the four autoionizing $(6p_j, 20s_{1/2})_J$ states of barium although the $(6p_j, 20s_{1/2})_{j\pm 1/2}$ pairs are separated by less than their autoionization linewidth. The energy and linewidth of each of the states have been measured. The $(6p_{1/2}, 20s_{1/2})_1$ state has an anomalous width which implies that it autoionizes primarily into excited $Ba^+(6p_{1/2})$ ions.

We report, to our knowledge, the first experimental resolution of pair splittings which are smaller than the autoionization linewidths in the autoionization spectrum of an atom. Specifically, we have measured the energies and linewidths of all four components belonging to the $(6p_j, 20s_{1/2})_J$ configuration in Ba. Previously, autoionizing states have been observed by single-photon vacuum-ultraviolet (vuv) absorption spectroscopy[1]; however, for alkaline-earth atoms, that technique is limited to only those states with a total angular momentum of 1. In a previous Letter,[2] we reported a three-step laser technique for populating autoionizing states of the $5p_j,ns$ configuration in strontium; however, only the gross splitting due to the $Sr^+(5p)$ fine structure was resolved. In the experiments reported here, we have made a significant refinement of our previous three-photon excitation scheme by using polarization techniques to force selective excitation of each individual J state, including the $J=0$ and 2 states which are inaccessible to single-photon vuv absorption studies. We have been able to measure the splittings between the $J=j+\frac{1}{2}$ state

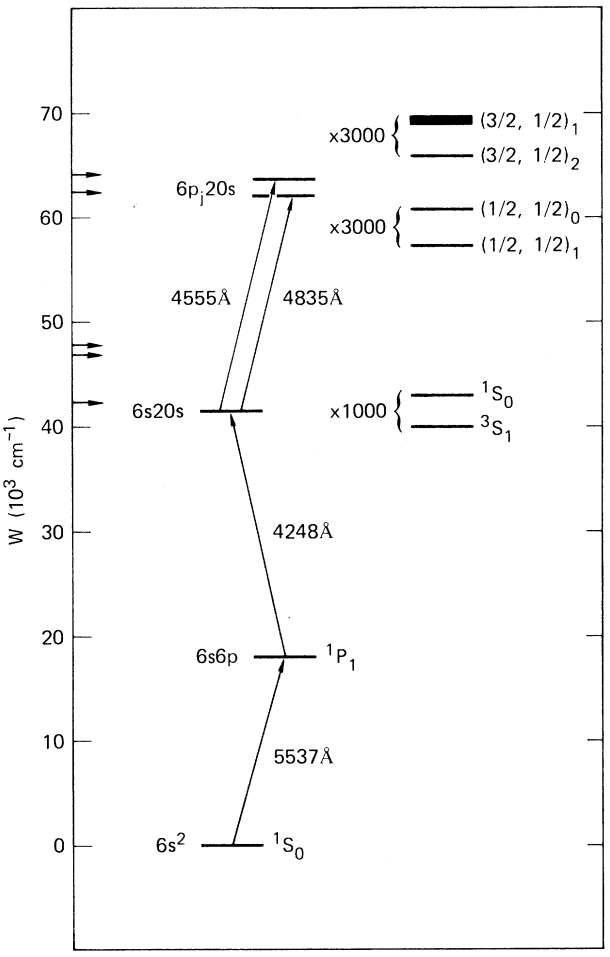

FIG. 1. Relevant energy levels for the excitation of the $(6p_j, 20s_{1/2})_J$ autoionizing states of Ba. The solid lines show the stepwise laser excitation. The expansions show the detailed splittings. The autoionizing states' linewidths are not shown to scale; however, the increased linewidth of the $(6p_{3/2}, 20s_{1/2})_1$ state is schematically illustrated. The arrows on the left-hand side represent the five lowest ionization limits, which correspond to Ba^+ in the $6s$, $5d_{3/2}$, $5d_{5/2}$, $6p_{1/2}$, and $6p_{3/2}$ states (from bottom to top).

and $J = j - \frac{1}{2}$ state for each $(6p_j, 20s_{1/2})_J$ pair, even though the splittings are smaller than the autoionization linewidths of the states.

In addition, we have also observed an anomalous linewidth for the $(6p_{3/2}, 20s)_1$ state, over 3 times as large as any of the other three states. We believe this increased linewidth is due to autoionization, mediated by a magnetic interaction, resulting in excited $Ba^+(6p_{1/2})$ ions. To our knowledge, this is also the first observation of autoionization via such an interaction. Since this process results in an optically inverted ion population, it may be useful for generating vuv or soft-x-ray lasers.[3] Furthermore, since this previously ignored autoionization process can be even faster than the normal autoionization to $Ba^+(6s)$ ions, this suggests that calculations of autoionization rates in other systems[4] (which are used to calculate dielectronic recombination rates) may be incomplete.

In Fig. 1 we show the relevant energy levels of Ba. The Ba is pumped stepwise, through the $6s6p\ ^1P_1$ state, to the $6s20s$ ($^1S_0$ or $^3S_1$) Rydberg state. The next excitation step does not affect the Rydberg electron, but only excites the remaining valence electron; thus, it corresponds to exciting the Ba^+ ion near one of the resonant transitions, $6s \rightarrow 6p_j$ (for simplicity, we will refer to the Rydberg electron as the "outer" electron, and to the other valence electron as the "inner" or "core" electron). This produces an autoionizing Rydberg state of the configuration $(6p_j, 20s_{1/2})_J$, where $j = \frac{1}{2}$ ($J = 0, 1$) or $j = \frac{3}{2}$ ($J = 1, 2$). By appropriate choice of the initial Rydberg state and of the core-excitation polarization, each of the four possible states can be populated individually.

The Ba is in an effusive atomic beam which passes into an interaction region between two parallel electric field plates. In this region the beam density is $\sim 10^8$ atoms/cm^3. The top field plate has a grid to allow ions to pass into an electron multiplier; the bottom plate can be pulsed to a high voltage in order to field ionize Rydberg states and drive the ions through the grid.

Three different choices of polarizations, which we shall label cases 1, 2, and 3, were used to populate the Rydberg $6s20s$ states. For the first case, both lasers were linearly polarized vertically. Then for each transition, $\Delta m_J = 0$ and therefore $|\Delta J| = 1$. The final state had to have even J, thus only the $^1S_0$ state was populated. For the second case, the first laser was polarized horizontally and the second vertically so that $|\Delta m_J| = 1$ for the first transition and $|\Delta m_J| = 0$ for the second transition. Then, since only $m_J = \pm 1$ final states could be populated, the $^1S_0$ state was not populated. For the third case, we used two oppositely circular polarized beams. This can produce final states of $m_J = 0$ for both $^1S_0$ and $^3S_1$. However, the energy splitting is sufficiently large (3.1 cm^{-1}), that we could set the laser to populate only the $^3S_1$. In this case, the quantization axis is along the direction of propagation.

The core-excitation laser was delayed by ap-

proximately 15 ns from the other lasers. To excite the core to the $6p_{1/2}$ state, its wavelength was near 4835 Å. To excite the core to the $6p_{3/2}$ state, its wavelength was near 4555 Å. For cases 1 and 2 above, it was nearly collinear with the other two lasers and was linearly polarized vertically. Since this produced $\Delta m_J = 0$, $|\Delta J| = 1$ transitions, case 1 resulted in $^1S_0 \rightarrow (6p_j, 20s_{1/2})_1$ transitions, and case 2 resulted in $^3S_1 \rightarrow (6p_{1/2}, 20s_{1/2})_0$ or $^3S_1 \rightarrow (6p_{3/2}, 20s_{1/2})_2$ transitions. For case 3, which was only used for the $p_{1/2}$ transitions, the third laser crossed the other two at a right angle in the interaction region. Since the Rydberg-state quantization axis in case 3 was in the direction of the first two lasers' propagation, the third laser polarization could be set either perpendicular to this axis ($|\Delta m| = 1$, final $m_J = \pm 1$) or parallel ($\Delta m = 0$, $|\Delta J| = 1$). This resulted in $^3S_1 \rightarrow (6p_{1/2}, 20s_{1/2})_1$ or $^3S_1 \rightarrow (6p_{1/2}, 20s_{1/2})_0$ transitions, respectively.

The wavelength of the core laser was calibrated using the spectroscopic data of Rubbmark, Borgström, and Bockasten.[5] Near the center of each wavelength scan, the third laser excited some of the $6s6p\ ^1P_1$ atoms to well-known Rydberg states ($5d6d\ ^3P_2$ at 4947 Å and $6s9d\ ^1D_2$ at 4557 Å) and subsequently photoionized them, resulting in a frequency marker, limited only by the laser linewidth. The laser scan rate was determined by splitting off and expanding 10% of the laser power and monitoring its transmission through a 3.0-cm^{-1} FSR (free-spectral range) etalon. This calibration technique worked best for the transition to the $p_{3/2}$ core, where the marker was only ~ 10 cm^{-1} from line center. In Fig. 2, the two transitions to the $p_{3/2}$ core are shown. The marker is plainly evident in both cases. For the $p_{1/2}$ core transitions, the marker was ~ 50 cm^{-1} from line center, seriously reducing the accuracy. This is why case-3 polarization (above) was used. Since the only laser change between transitions to $(6p_{1/2}, 20s_{1/2})_1$ and $(6p_{1/2}, 20s_{1/2})_0$ was the rotation of a polarizer in the core laser path, the etalon itself could be used as an absolute frequency marker by recording its transmission simultaneously with the ion signal. We determined that the etalon frequency markers were stable to 0.2 cm^{-1} over several cycles of wavelength scan by alternating between the two transitions.

The third laser power was adjusted by putting neutral density filters in its path. To avoid power broadening, we reduced the power until the ion signal decreased linearly with laser power.

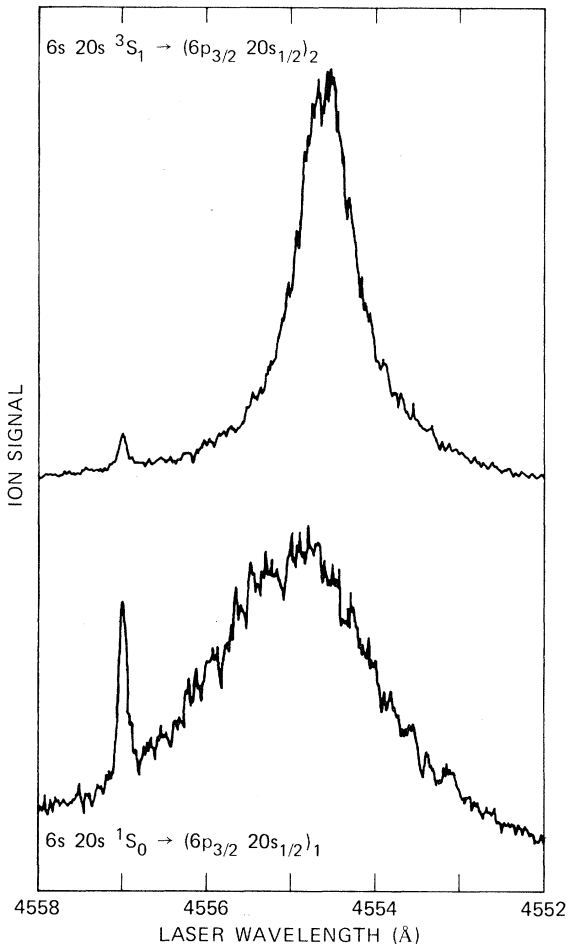

FIG. 2. Excitation spectra of the two $(6p_{3/2}, 20s_{1/2})_J$ states. In each spectrum, the sharp peak corresponds to excitation of the $6s9d\ ^1D_2$ Rydberg state of Ba, and thus serves as a convenient frequency marker. Since the $^3S_1$ Rydberg state lies 3.1 cm^{-1} (0.64 Å) below the $^1S_0$ state, the true energy ordering of the autoionizing states is the opposite of the ordering in these spectra.

Data were typically taken at a laser power reduced further by 50%. For the $p_{1/2}$ core case, the laser power was increased temporarily as the laser scanned over the marker region, to enhance its visibility.

Table I lists the energies and the widths of the four $(6p_j, 20s_{1/2})_J$ states. The accuracy of the energy measurements is limited primarily by wavelength measurements. We estimate the Fano q parameter[6] for even the broadest line to be 10^3 (using 3×10^{-15} cm^2 for the autoionization-broadened resonance absorption cross section, and 10^{-21} cm^2 for the direct Rydberg photoionization cross section[7]). For such large q, the apparent line shift should be only 10^{-2} cm^{-1}. The effective

TABLE I. Energies and linewidths of $(6p_j, 20s_{1/2})_J$ states of barium.

j	J	W (cm^{-1})	Γ(FWHM) (cm^{-1})
3/2	1	63 543.5(3)	11.0(5)
3/2	2	63 542.2(3)	3.1(5)
1/2	0	61 853.4(4)	3.0(5)
1/2	1	61 852.3(4)	3.0(5)

laser line shape (measured by tuning the laser through a marker resonance) was not so well behaved; it depended strongly on the dye used and laser-cavity alignment. Typically, the width was 0.5 cm^{-1} for the 4835-Å transition, and 1 cm^{-1} for the 4555-Å transition.

From Table I, one can see that the fine-structure doublets have the same ordering and approximately the same-size splitting. If these splittings were due to the $\vec{S}_1 \cdot \vec{S}_2$ interaction, resulting from the exchange portion of the electrostatic interaction between the two electrons, $1/r_{12}$, then the lower doublet would have half the separation and inverted order.[8] This leads us to believe that the splitting is due to a spin–outer-orbit interaction.[8] One can expect that the Rydberg electron spin density near the core would result in a splitting of the order of the $6p$ fine structure reduced to $[2/(n^*)^3](1690\ cm^{-1}) \approx 0.9\ cm^{-1}$.

This proposed $\vec{S}_2 \cdot \vec{L}_1$ coupling ("2" refers to the Rydberg electron, "1" refers to the core electron) can also lead to autoionization through an additional channel. Since the $(6p_{3/2}, 20s_{1/2})_1$ state lies above the $6p_{1/2}$ continuum, any coupling which tends to break down the coupling of $\vec{S}_1$ to $\vec{L}_1$ can lead to autoionization to the $(6p_{1/2}, \epsilon s_{1/2})_1$ continuum state. Since there does not exist a $(6p_{1/2}, \epsilon s_{1/2})_2$ continuum state, this autoionization channel is not open to the $(6p_{3/2}, 20s_{1/2})_2$ state. Both $(6p_{1/2}, 20s_{1/2})_J$ states do not have sufficient energy to autoionize into any $(6p_j, \epsilon s_{1/2})_J$ continuum states. Thus, this autoionization channel, into an excited $6p$ core state, will only increase the linewidth of the $(6p_{3/2}, 20s_{1/2})_1$ state.

Following the procedure outlined by Fano,[6] we can estimate the contribution this channel will make to the total autoionization rate. In particular, if an $\vec{S}_2 \cdot \vec{L}_1$ interaction results in a splitting Δ, then it will also result in first-order perturbed wave functions:

$$|6p_{3/2}, ns_{1/2}\rangle_1 = |6p_{3/2}, ns_{1/2}\rangle_1 + \sum_{n_1} \left(\frac{n^*}{n_1^*}\right)^{3/2} \frac{\Delta}{\sqrt{2}} \frac{1}{[\epsilon + 0.5/(n_1^*)^2]} |6p_{1/2}, n_1 s_{1/2}\rangle_1, \quad (1)$$

where ϵ is the energy of the autoionizing Rydberg state above the $6p_{1/2}$ ionization limit. But now the $|6p_{1/2}, n_1 s_{1/2}\rangle_1$ character can be coupled to the $|6p_{1/2}, \epsilon s_{1/2}\rangle_1$ continuum wave functions through the very strong scalar portion of the electrostatic $1/r_{12}$ force resulting in an autoionization width:

$$\Gamma(\text{FWHM}) \approx 12\pi (n^*)^3 \Delta^2 (\ln\epsilon/E_b)^2 \text{ a.u.} \approx 9\ cm^{-1}. \quad (2)$$

(FWHM is full width at half maximum.) This result was obtained by making the rough approximation that near its probability maximum, the bound-state wave-function amplitude $[2(3n_1^*)^{1/2}]^{-1}$ times that of the continuum wave function.[9] The excellent agreement is no doubt fortuitous; but, this estimation does illustrate that a 1-cm^{-1} splitting can imply a somewhat larger autoionization linewidth. Equation (2) shows that the autoionization rate scales as the square of the fine splitting. This is presumably the reason why it was not observed in our earlier studies of strontium, where the ionic fine structure is 10 times smaller.

In conclusion, we have resolved autoionizing states of Ba even though the states are separated by less than their autoionization linewidths. Furthermore, the anomalous linewidth of the $(6p_{3/2}, 20s_{1/2})_1$ state implies the existence of a new autoionization mechanism which results in the production of optically excited ions. Both of these results should provide important checks on calculations of multielectron wave functions.

This work was supported partially by internal SRI International funds and partially by the National Science Foundation under Grant No. PHY76-24541. We would like to acknowledge useful discussions with R. D. Cowan and D. L. Huestis during the analysis of this work.

[1]See, for example, W. R. S. Garton and K. Codling, Proc. Phys. Soc. London 75, 87 (1960); or, for recent work on BaI, C. M. Brown and M. L. Ginter, J. Opt. Soc. Am. 68, 817 (1978).

[2]W. E. Cooke, T. F. Gallagher, S. A. Edelstein, and R. M. Hill, Phys. Rev. Lett. 40, 178 (1978).

[3]S. E. Harris, private communication.

[4]See, for example, A. L. Merts, R. D. Cowan, and H. H. Magee, Jr., Los Alamos Scientific Laboratory Informal Report No. LA-6220-MS, 1976 (unpublished).

[5]J. R. Rubbmark, S. A. Borgström, and K. Bockasten, J. Phys. B 10, 421 (1977).

[6]U. Fano, Phys. Rev. 124, 1866 (1961).

[7]D. C. Lorents, D. J. Eckstrom, and D. L. Huestis, SRI International Final Report No. MP 73-2, 1973 (unpublished).

[8]E. U. Condon and G. H. Shortley, *The Theory of Atomic Spectra* (Cambridge Univ. Press, Oxford, 1935).

[9]Continuum wave functions and their normalization are discussed in H. A. Bethe and E. E. Salpeter, *Quantum Mechanics of One and Two Electron Atoms* (Academic, New York, 1957). Rydberg, low-l, wave functions have a peak in probability density, centered at $1.5(n^*)^2$, with a width of $3n^*$, as illustrated in Ref. 7.

Lamb Shift and Fine Structure of $n=2$ in ^{35}Cl XVI

H. G. Berry, R. DeSerio, and A. E. Livingston[a]

Argonne National Laboratory, Argonne, Illinois 60439, and Department of Physics, University of Chicago, Chicago, Illinois 60637

(Received 14 August 1978)

We have measured the wavelengths of the $2s\ ^3S_1-2p\ ^3P_2$ and $2s\ ^3S_1-2p\ ^3P_0$ transitions in Cl XVI to be 613.825±0.013 Å and 705.854±0.076 Å. Our precision is sufficient to provide measurements of the $2s_{1/2}-2p_{1/2}$ and $2s_{1/2}-2p_{3/2}$ Lamb shifts to an accuracy of ±0.3% and to test quantum electrodynamics (QED) theory in the strong-field region. We compare our results with the one-electron QED theories of Mohr and Erickson and discuss the accuracy of calculations of electron correlation in two-electron atoms.

We wish to emphasize in this paper that Lamb-shift measurements in high-Z atoms need not be confined to the one-electron hydrogenic ions, but higher precision may be attainable in ions with a few (two or three) electrons. We present a measurement in two-electron chlorine to justify this suggestion and discuss briefly the limitations in the precision of such measurements due to the accuracy of calculations of relativistic energies in many-electron atoms.

In two-electron ions of low Z ($Z \lesssim 10$), there have been several experimental tests[1] of quantum electrodynamics, but of lower precision than measurements in the corresponding one-electron atoms. Electron correlation effects have been calculated approximately to first order in the Lamb-shift terms[2] and less accurately than the experimental values.[3] However, such effects become less important at high Z since the correlations can be expressed as part of a $1/Z$ expansion.

Tests of quantum electrodynamics by $2s$-$2p$ Lamb-shift measurements in one-electron atoms have been reviewed recently by Kugel and Murnick[4] and by Mohr.[5] They point out that although the highest-precision measurements are in hydrogen (20 ppm),[6] the higher-order terms of the Lamb shift, which is usually expressed as a power series expansion in $Z\alpha$, are more easily tested in higher-Z ions. The present most precise measurements are those in $^{19}F^{8+}$ ($Z=9$)[7] and $^{40}Ar^{17+}$ ($Z=18$)[8] of ±2% and ±4% accuracy, respectively, both of which test the higher-order terms of the Lamb shift to approximately the same accuracy as the work in hydrogen.[6] The higher-order terms in $Z\alpha$ probe quantum electrodynamic (QED) theory in strong fields where the perturbative theory must eventually break down. Comparable tests occur only in the comparisons between theory and experiment of the binding energy of K-shell electrons in high-Z atoms,[9] where an accuracy of about 10% has been achieved. Davis and Marrus[10] measured the two-electron Lamb shift in Ar XVII, but only with low precision (~±30%).

We accelerated chlorine ions in the Argonne FN tandem accelerator to an energy of 80 MeV and further stripped and excited the ion beam in a thin 20-μg-cm^{-2} carbon foil. The observation angle (close to 90°) was deduced from the relative Doppler shifts at beam energies between 56 and 88 MeV. Thus, the first- and second-order Doppler shifts are ~3 Å/deg and ~3 Å, respectively, at 1200 Å for 80 MeV ion beam energy. As we were able to use internal calibration lines in the beam-foil spectra, such Doppler shifts had very little effect on the values of our measured wavelengths. The monochromator was refocused for the fast-moving light source ($v/c=\beta\sim 0.07$) by adjustment of both the entrance slit and the grating.[11]

In Fig. 1, we show wavelength scans including